

# EPR Study of CO and O<sub>2</sub> Interaction with Supported Au Catalysts

Mitsutaka Okumura,\* Juan M. Coronado,† Javier Soria,† Masatake Haruta,\* and José C. Conesa†<sup>1</sup>

\* Osaka National Research Institute, AIST MITI, Midorigaoka 1-8-1, Ikeda 563-8577, Japan; and † Instituto de Catálisis y Petroleoquímica, CSIC, Campus de Cantoblanco, 28049 Madrid, Spain

Received March 14, 2001; revised June 13, 2001; accepted June 18, 2001

The interaction of CO and O<sub>2</sub> with Au/TiO<sub>2</sub> and Au/Al<sub>2</sub>O<sub>3</sub> catalysts is studied with EPR spectroscopy. Adsorption of CO and O<sub>2</sub> can produce at room temperature in both fresh catalysts O<sub>2</sub><sup>-</sup> radicals stabilized on support cations (suggesting a spillover process exists at least in Au/Al<sub>2</sub>O<sub>3</sub>); thus, O<sub>2</sub><sup>-</sup> generation does not require a reducible support. These O<sub>2</sub><sup>-</sup> species react upon CO addition giving diamagnetic species. CO adsorption at room temperature on freshly activated Au/TiO<sub>2</sub> abstracts oxygen ions from the support surface producing Ti<sup>3+</sup> anion vacancy centers, but after the specimen has interacted with both O<sub>2</sub> and CO a new CO adsorption gives (reversibly, suggesting easy Au–titania electronic interaction) only fully coordinated Ti<sup>3+</sup> unable to stabilize O<sub>2</sub><sup>-</sup>; this indicates coverage of Ti active centers by reaction products (e.g., carbonate or peroxide species) which are not eliminated by CO or O<sub>2</sub>. The results indicate that steady state catalytic CO oxidation on Au/TiO<sub>2</sub> may proceed without involving Ti-stabilized O<sub>2</sub><sup>-</sup>. © 2001 Academic Press

**Key Words:** gold catalysts; TiO<sub>2</sub>; CO oxidation; EPR spectroscopy; superoxide radicals.

## INTRODUCTION

In recent years gold has been shown to have surprisingly high activity at low temperatures for CO oxidation when it is deposited as nanoparticles on selected metal oxides (1–4). Coprecipitation (2, 5, 6), deposition–precipitation (1, 7), cosputtering (8), gas-phase grafting (3), and liquid-phase grafting methods (4) can produce highly dispersed gold catalysts, which exhibit unique catalytic features in many different reactions depending on the type of metal oxide supports (9). In the case of CO oxidation, the use as supports of oxides of several 3d transition metals and hydroxides of alkaline earth metals (10) leads to high activities even at temperatures as low as 203 K. Although quite unique catalytic activities have been reported for such gold catalysts, neither the reaction mechanism of CO oxidation nor the active oxygen species operating over them have been elucidated unambiguously.

EPR is a highly sensitive technique that is very suitable to study redox processes, especially when involving transition metal oxides (including catalytic materials) and/or single electron transfer steps. In particular, it gives well-resolved signals allowing us to discriminate among several kinds of species in the case of reduced Ti ions (11) and oxygen-derived adsorbed radicals, which can be used as valuable probes to explore the state of oxide surfaces (12, 13). Here it has been used as a tool helping to clarify reaction steps involved in CO oxidation over titania- and alumina-dispersed gold catalysts.

## EXPERIMENTAL

An Au/TiO<sub>2</sub> catalyst was prepared by the deposition–precipitation method. For this, a 1 mmol/l solution of HAuCl<sub>4</sub> in distilled water was adjusted to pH 7 by adding NaOH, and TiO<sub>2</sub> (Degussa P-25, specific surface area 50 m<sup>2</sup>/g, mainly anatase but containing ca. 30% rutile) was added to it, the suspension being subsequently aged at 343 K for 1 h. The solid was filtered and repeatedly washed with distilled water, dried under vacuum, and calcined at 673 K in air for 4 h; the final Au content amounted to 1 wt%. The resulting mean diameter of the TiO<sub>2</sub>-deposited Au particles obtained was estimated by TEM to be 3.3 ± 0.6 nm. For comparison purposes, a chloride-treated titania sample (without gold) was prepared by following the same procedure but using HCl instead of HAuCl<sub>4</sub>.

The preparation of Au/Al<sub>2</sub>O<sub>3</sub>, via a gas-phase grafting method, used as gold source (CH<sub>3</sub>)<sub>2</sub>Au(CH<sub>3</sub>COCH<sub>2</sub>COCH<sub>3</sub>), abbreviated as Me<sub>2</sub>Au(acac) (Tri Chemical Laboratory), and as support a γ-Al<sub>2</sub>O<sub>3</sub> reference sample of the Catalysis Society of Japan (JRC-ALO-7, specific surface area 180 m<sup>2</sup>/g). The latter was evacuated at 473 K for 4 h (ultimate pressure about 10<sup>-3</sup> Torr; 1 Torr = 133.3 N m<sup>-2</sup>) to remove physically adsorbed water, and then treated with 20 Torr of O<sub>2</sub> at 473 K for 30 min to remove organic residues and oxidize the surface. The Me<sub>2</sub>Au(acac)-containing vessel, connected to the same vacuum line, was heated to a fixed temperature of 306 K in order to gradually evaporate a measured amount of Au compound and adsorb it on the support kept at 303 K; the solid was finally calcined in

<sup>1</sup> To whom correspondence should be addressed. E-mail: [jconesa@icp.csic.es](mailto:jconesa@icp.csic.es).

air at 673 K to decompose the Au precursor into metallic gold particles, resulting in an Au load of 3 wt% and a mean particle diameter (TEM data) of  $3.5 \pm 2.7$  nm.

Electron paramagnetic resonance (EPR) spectra were recorded at 77 K with a Bruker ER 200D spectrometer working in the X-band and calibrated with a DPPH standard ( $g = 2.0036$ ). Weighted portions of 20–40 mg of catalyst were placed inside a quartz probe cell with greaseless stopcocks. A conventional dynamic high-vacuum line was used for vacuum treatments and gas adsorption. In all cases the samples were initially subjected in the quartz cell to the following standard pretreatment: evacuation for 1 h at 523 K ( $p < 3 \times 10^{-4}$  Torr), calcination in static  $O_2$  atmosphere (ca. 200 Torr) at the same temperature for 30 min, and cooling under  $O_2$ , followed by outgassing at room temperature (RT) to eliminate excess oxygen. A specimen pretreated *in situ* in this way is called “fresh sample.” Unless stated otherwise, evacuations were always carried out for the time necessary to achieve the  $3 \times 10^{-4}$  Torr reference value. Gas adsorption was carried out by expanding over the sample a fixed volume of gas ( $\approx 5$  ml) prefilled with a known pressure (20 Torr) of the latter. In the case of oxygen adsorption a final outgassing treatment at 77 K was always carried out to remove any physisorbed excess  $O_2$ , which could lead to dipolar magnetic broadening of the signals. In all spectra reported the vertical amplitudes are normalized to the same sample weight.

## RESULTS

### Oxygen Adsorption on Prereduced Samples

The fresh  $TiO_2$  sample presents rather weak EPR signals (Fig. 1a). Outgassing at high temperature (673 K) generates strong  $Ti^{3+}$  signals (Fig. 1b). The main one, with extrema at  $g = 1.966$  ( $g_{\perp}$ -type feature) and  $g = 1.949$  ( $g_{\parallel}$ -type feature), is due to surface  $Ti^{3+}$  ions having in their coordination sphere anion vacancies (generated by  $O_2$  desorption) (11); a narrower peak at  $g = 1.991$  ( $g_{\perp}$ -type feature) is due to reduced centers (probably bulk defects) in anatase (14). A small symmetric signal  $S$  also appears at  $g = 2.002$ , which may be due to electrons trapped at bulk anion vacancy defects or to organic radicals (formed, e.g., from incompletely burnt adsorbed contaminant molecules); some results (see below) seem to favor the first explanation.

Subsequent  $O_2$  adsorption at RT (Fig. 1c) leads to the disappearance of the main  $Ti^{3+}$  signals; a small peak remains at  $g = 1.978$ , which might be present already in the spectrum of Fig. 1b (as well as in the initial spectrum of Fig. 1a, albeit with smaller intensity) and can be due to bulk  $Ti^{3+}$  centers without vacancies in the coordination sphere (defects) in rutile (11) (this latter phase is present in the P25 material in ca. 30% amounts). Simultaneously, new features appear at  $g = 2.025$  and 2.009 which can be ascribed to  $O_2^-$  radicals

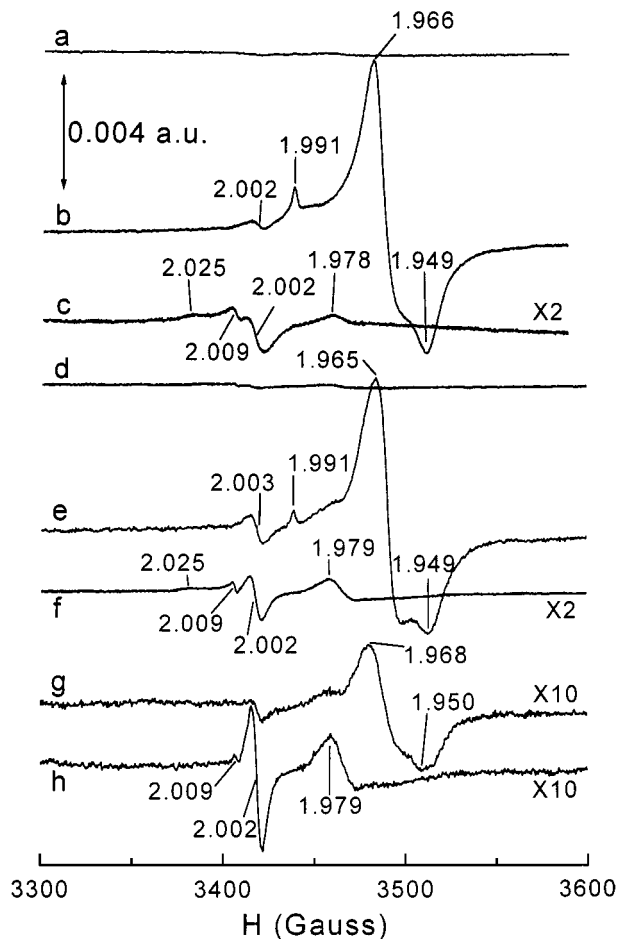


FIG. 1. EPR spectra (at 77 K) of oxygen adsorption on reduced samples: (a) spectrum of fresh  $TiO_2$ ; (b) after outgassing it at 673 K for 1 h; (c) after subsequent  $O_2$  adsorption (15 Torr) at RT. (d–f) Same experiments on fresh Au/ $TiO_2$  sample. For a fresh Au/ $TiO_2$  sample: (g) after contacting with CO (one 20 Torr dose) at RT; (h) after subsequent brief outgassing and exposure to  $O_2$  at RT.

stabilized on surface  $Ti^{4+}$  ions (12); the third  $g$  value of this species, expected to be close to  $g = 2.002$ , is obscured by its overlap with the symmetric signal  $S$ , located at the same position and little changed by  $O_2$  adsorption.

For the Au/ $TiO_2$  catalyst, the behavior observed, depicted in Figs. 1d–1f, is rather similar. Here the strong  $Ti^{3+}$  signal formed upon outgassing at 673 K (Fig. 1e) appears with somewhat less sharp features and similar amplitude to that found in pure  $TiO_2$ . After  $O_2$  adsorption (Fig. 1f) the amount of  $O_2^-$  radicals formed is also relatively similar, as ascertained from the features at  $g = 2.009$  and 2.025 (the  $O_2^-$  feature expected near  $g = 2.002$  is again obscured by signal  $S$ , which though decreased appreciably upon  $O_2$  adsorption remains still larger than in the pure titania sample); the signal at  $g = 1.979$  due to bulk  $Ti^{3+}$  defects appears with higher intensity (ca. 3 times larger) than for pure titania. It is noted that if the same treatment is applied to

the chloride-treated TiO<sub>2</sub> sample these two latter signals appear also larger than in the parent titania material (spectra not shown), evidencing that their higher intensity observed in the Au/TiO<sub>2</sub> sample is not necessarily related directly to the added gold component. It must be pointed out also that in all these samples the amount of O<sub>2</sub><sup>-</sup> species formed is much smaller than the amount of Ti<sup>3+</sup> ions which disappear upon O<sub>2</sub> adsorption (as judged from the doubly integrated intensities of the respective signals); thus, this elimination of Ti<sup>3+</sup> by O<sub>2</sub> addition must correspond mostly to the formation of diamagnetic oxygen anions (O<sub>2</sub><sup>2-</sup> or O<sup>2-</sup>).

The adsorption of CO at RT on a fresh Au/TiO<sub>2</sub> sample leads also to significant reduction: it produces mainly a signal (Fig. 1g) with extrema at  $g = 1.968$  and  $1.950$ , similar (although in lower amount) to that generated by outgassing at 673 K (Fig. 1e) and ascribable also to surface Ti<sup>3+</sup> ions with coordination vacancies. Again this Ti<sup>3+</sup> signal disappears when, after outgassing at RT the unreacted CO, O<sub>2</sub> is adsorbed on the sample at RT (Fig. 1h). A small amount of O<sub>2</sub><sup>-</sup> radicals is then detected as indicated by the sharp feature at  $g = 2.009$ ; the proportion between the amount of this species and that of the Ti<sup>3+</sup> eliminated seems similar to that observed in the experiments of Figs. 1e and 1f. Apart from this, O<sub>2</sub> adsorption produces a significant increase in the symmetric signal *S* and in the bulk Ti<sup>3+</sup> component at  $g = 1.979$ . In contrast with the behavior of samples outgassed at 673 K, it must be mentioned that these latter processes occurring upon interaction with CO at RT require the presence of Au: no EPR signal appears on fresh pure TiO<sub>2</sub> after CO adsorption, nor upon subsequent O<sub>2</sub> adsorption at 77 K or RT (spectra not shown).

#### Interaction with CO and O<sub>2</sub>

In the Au/TiO<sub>2</sub> catalyst, CO adsorption (one 20 Torr dose) at 77 K on the fresh sample leads to a significant generation of bulk Ti<sup>3+</sup> species (Figs. 2a and 2b), although in amounts somewhat lower (ca. 3 times) than that of the Ti<sup>3+</sup> formed at RT (Fig. 1g). Subsequent addition of O<sub>2</sub> (also one 20 Torr dose) at 77 K causes no change in the spectrum, but warming of the sample cell at RT after this leads to the appearance of a sharp signal, with  $g$  values 2.002, 2.009, and 2.025 (Fig. 2c), typical of O<sub>2</sub><sup>-</sup> radicals bonded to Ti<sup>4+</sup> ions; it is noted that the bulk Ti<sup>3+</sup> signal at  $g = 1.979$  is hardly changed. Tests of the thermal evolution of this O<sub>2</sub><sup>-</sup> species were carried out in separate runs, in which after generating its signal (e.g., as in Fig. 2c) the sample was warmed in the closed EPR cell at different temperatures above RT. In those experiments (spectra not shown) the signal intensity decreased slightly (ca. 20%) by warming at 323 K, and more markedly (nearly fourfold) at 373 K, vanishing when heating at higher temperatures; nearly no change occurs in the bulk Ti<sup>3+</sup> signal along this process. The O<sub>2</sub><sup>-</sup> signal formed in the experiment of Fig. 2c is not modified (except for some broadening) by

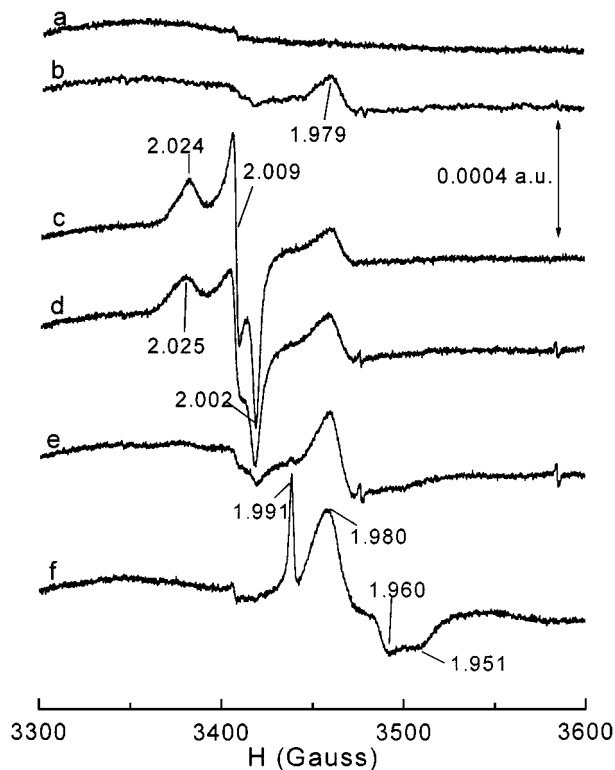


FIG. 2. EPR spectra at 77 K obtained on Au/TiO<sub>2</sub>: (a) fresh sample; (b) contacted with CO (one 20 Torr dose); (c) after addition of O<sub>2</sub> (one 20 Torr dose) at 77 K and subsequent warming at RT for 6 min; (d) after introduction into the cell (without any evacuation) and a second 20 Torr dose of CO at 77 K; (e) subsequent warming to ca. 273 K for less than 1 min; (f) after evacuation and addition of a new dose of CO (20 Torr) at RT.

addition of another 20 Torr dose of CO at 77 K (Fig. 2d), but brief warming to near room temperature in the presence of this newly added CO eliminates most of the O<sub>2</sub><sup>-</sup> species (Fig. 2e), which completely disappear upon addition of new CO doses at RT, while Ti<sup>3+</sup> species do grow significantly (Fig. 2f).

From this moment on, the Ti<sup>3+</sup> signals increase further in intensity upon extended contact with CO (Figs. 3a and 3b). Several different Ti<sup>3+</sup> centers appear in these latter spectra. The characteristic anatase signal at  $g = 1.991$  is one of them, while the largest feature coincides in position with the mentioned bulk defect centers at  $g = 1.979$ , although its intensity, rather larger than that observed in the previous experiments, makes it doubtful that here it may be due just to bulk defects. Other species appear in addition, as revealed by a somewhat broader peak at ca.  $g = 1.985$  (better ascertained after outgassing, see below) and by a wide component with minimum feature at ca.  $g = 1.91$ , which must be ascribed also to Ti<sup>3+</sup> species. For the signals at  $g = 1.979$  and  $1.985$  the titanium cations probably retain a high coordination number, considering the deviations of their main  $g$  feature from the free electron  $g$  value

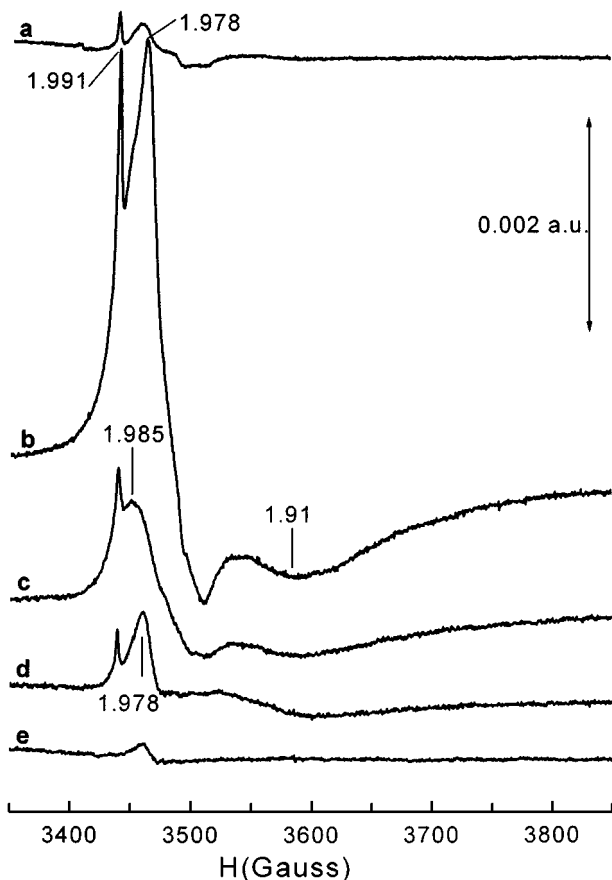


FIG. 3. EPR spectra at 77 K obtained on Au/TiO<sub>2</sub> previously contacted with CO and O<sub>2</sub>: (a) same spectrum as in Fig. 2f; (b) after outgassing at RT and adsorption of a new dose of CO (20 Torr) at RT for 12 h; (c) after evacuation at RT; (d) contacted with one dose (20 Torr) of O<sub>2</sub> at 77 K, (e) then warmed at RT for ca. 1 min.

$g_e = 2.0023$ , which are relatively small in comparison to that observed in Figs. 1b and 2b where the signal is ascribed to Ti<sup>3+</sup> ions with vacancies in their coordination sphere; one should recall that, to a first approximation, the magnitude of these deviations is inversely related to the ligand field strength (15). The assignment of the signal responsible for the feature at  $g = 1.91$ , for which the position of the lower field feature(s) cannot be determined unambiguously, is less clear; neither its coordination degree nor the reasons for its large linewidth can be ascertained clearly.

This generation of Ti<sup>3+</sup> is partially reversed by outgassing at RT (Fig. 3c), the feature at ca.  $g = 1.985$  being now resolved more clearly. Subsequent addition of O<sub>2</sub> on the sample, even at low temperature (77 K), leads to a significant decrease in the Ti signal (Fig. 3d); the signals at  $g = 1.991$  and 1.979, typically ascribed to bulk Ti<sup>3+</sup>, are the least affected ones. These latter signals do nearly disappear if the sample is brought into contact with O<sub>2</sub> at room temperature (Fig. 3e). It is noteworthy that in all these latter experiments involv-

ing a new oxygen adsorption no O<sub>2</sub><sup>-</sup> radicals appear in the spectrum.

#### Behavior of Au/Al<sub>2</sub>O<sub>3</sub>

In a comparative experiment, the behavior of the Au/Al<sub>2</sub>O<sub>3</sub> catalyst was examined. As expected, no support-related defect center was detected by EPR in different reduction experiments. However, a paramagnetic species did appear when the fresh sample, after adding to it (stepwise) CO and O<sub>2</sub> at 77 K, was warmed for 5 min at RT (Fig. 4b). This signal, for which computer simulation gave parameters  $g = 2.001, 2.010, 2.040$ , is similar to that assigned in the literature to O<sub>2</sub><sup>-</sup> radicals stabilized on Al cations (16), the relatively broadened shape being ascribable to an unresolved hyperfine splitting (interaction of the unpaired electron with the magnetic Al nucleus). Double integration of the spectra showed that the amount of these radicals appearing in Fig. 4b is somewhat larger (nearly 40%) than that found on Au/TiO<sub>2</sub> in a comparable experiment (Fig. 2c). The intensity of this signal increased significantly by warming the sample in the closed EPR cell at  $T = 323$  K (Fig. 4c); warming at  $T = 373$  K led to a small decrease (Fig. 4d), and the signal vanished upon heating at higher temperatures.

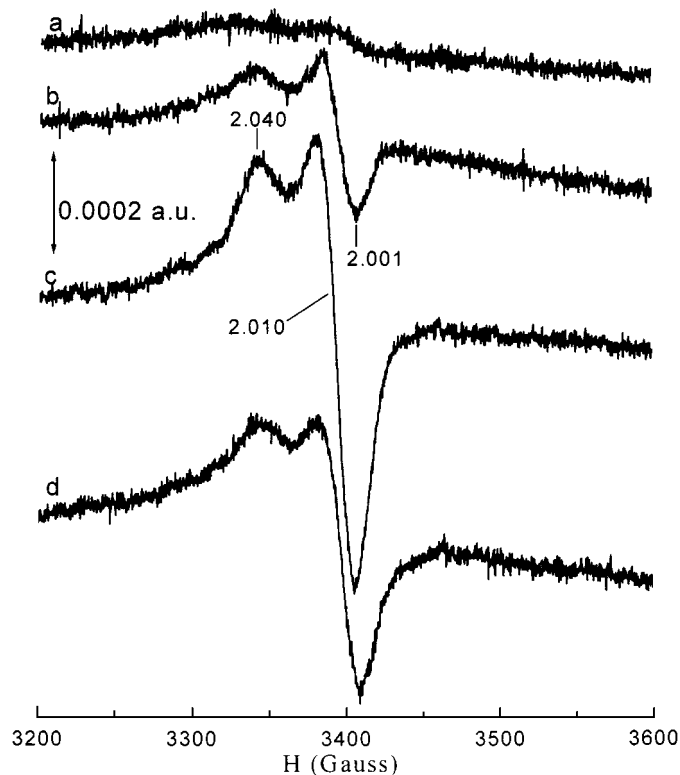
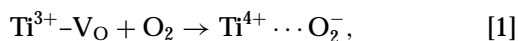


FIG. 4. EPR spectra at 77 K obtained on Au/Al<sub>2</sub>O<sub>3</sub>: (a) fresh sample; (b) contacted at 77 K stepwise with CO and O<sub>2</sub> (one dose of 20 Torr each), and then warmed briefly (5 min) at RT; (c) warmed for 5 min at 323 K and (d) at 373 K.

## DISCUSSION

*The Role of the Support in the Generation of  $O_2^-$* 

The formation of Ti-bonded  $O_2^-$  species upon  $O_2$  adsorption on titania-based materials previously subjected to reduction is a well-known observation, normally interpreted as due to an electron transfer process,

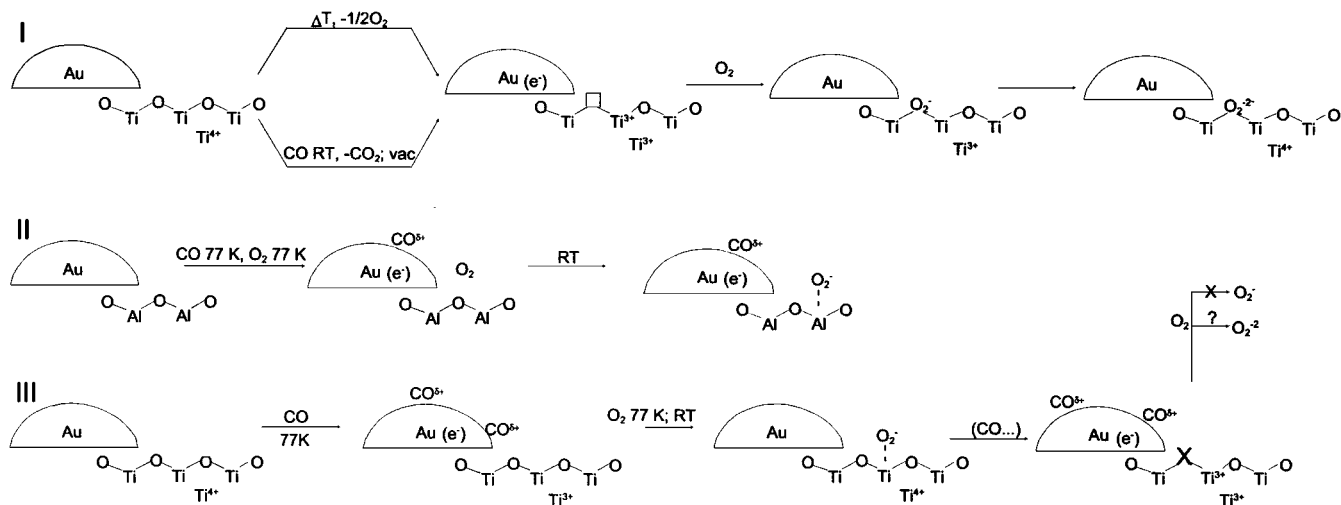


where  $V_O$  represents an oxygen vacancy at the Ti coordination sphere and the resulting  $O_2^-$  remains stabilized on the vacancy. This may be eventually followed by further electron transfer yielding  $O_2^{2-}$  and finally (after O-O bond scission)  $O^{2-}$ . This is depicted graphically in line I (upper branch) of Scheme 1 for the simpler case of reduction through thermal treatment. The generation of the  $O_2^-$  radicals appearing in Figs. 1c and 1f may be interpreted in this way, and the similarity of the results obtained in this case for the bare  $TiO_2$  support and the  $Au/TiO_2$  catalyst indicates that the presence of the metal does not seem to create any special new type of centers for this process; i.e., the  $Ti^{3+}-V_O$  and  $O_2^-$  species formed in the catalyst do not differ substantially from those expected for the normal titania surface.

The results obtained upon contact of the  $Au/TiO_2$  sample with CO at RT (Fig. 1g) show that this interaction reduces the titania support, precisely by eliminating surface oxygen ions, since the  $Ti^{3+}$  centers formed are of the same type associated with surface vacancies as mentioned above; this is represented in line I (lower branch) of Scheme 1. No such result is observed when CO interacts with Au-free titania, showing that CO activation by the Au particle is needed for this. Quite probably this process

remains limited to the titania surface sites closest to the Au particles, in agreement with the relatively small number of reduced centers formed, rather lower than that achieved by outgassing at 673 K. It is noted that adsorption of  $O_2$  at RT produces an effect rather similar to that in the case of the samples reduced by outgassing at 673 K: the  $Ti^{3+}$  vacancy centers vanish and a small amount of  $O_2^-$  remains (in nearly the same proportion to the initial  $Ti^{3+}$  as in the cases of reduction by outgassing). Again, the  $Ti^{3+}$  centers appearing in these processes on  $Au/TiO_2$  do not seem to have any characteristic significantly different from those which can be formed on titania alone; at most, one notes a somewhat broader shape which might be due to some interaction of these centers with the nearby metal particle.

The observation of Al-bonded  $O_2^-$  in the  $Au/Al_2O_3$  catalyst (Fig. 4), however, is hard to explain with this scheme, as neither  $Al^{2+}$  nor any other reduced alumina species is expected to exist under these conditions. One must assume that the electron transfer to the  $O_2$  molecule occurs directly from the Au particle, in a process somehow stimulated by CO. Possibly, the adsorption of CO raises the Fermi level of the metal so that transfer of an electron to give  $O_2^-$  becomes feasible; this radical is then stabilized on a neighboring  $Al^{3+}$  ion. This is depicted briefly in line II of Scheme 1. Here it is not clear whether the  $O_2^-$  radical forms on the Au particle itself, and then migrates to the support (a spillover phenomenon), or the electron transfer occurs while the  $O_2$  molecule is weakly adsorbed on the alumina surface at points close to the metal; this second alternative is the one represented in Scheme 1. The overall process, in any case, seems to require in this material a significant thermal activation, since the amount of those radicals increases when the temperature is raised above ambient. Depending on the mechanism model, this activation energy would correspond



SCHEME 1

to the electron transfer itself or to the diffusion of the previously formed radicals onto and over the alumina surface.

Since  $O_2^-$  can be formed on Au/Al<sub>2</sub>O<sub>3</sub> in this way, for Au/TiO<sub>2</sub> it is no longer certain whether, in the situation of Fig. 2, these radicals are formed with the intervention of surface Ti<sup>3+</sup> species as described by Eq. [1]. For the experiments of Figs. 2 and 4 the overall amount of  $O_2^-$  radicals detected is not much different (note that the way in which CO and O<sub>2</sub> are added is identical in both cases), suggesting that their mechanism of formation in the CO + O<sub>2</sub> reaction is similar. One notes, however, that for Au/TiO<sub>2</sub> warming at 323 K does not increase the  $O_2^-$  signal, which contrasts with the behavior observed for Au/Al<sub>2</sub>O<sub>3</sub> and suggests that a smaller activation energy is needed; this could be related to a specific facilitation of the electron transfer through Ti ions.

#### *Metal-to-Support Electron Transfer in Au/TiO<sub>2</sub>*

An interesting observation is that in the experiments reflected in Fig. 3, involving a sample already contacted with CO and O<sub>2</sub>, CO adsorption produces an increase in the amount of Ti<sup>3+</sup> species (Figs. 3a and 3b), now not associated with anion vacancy generation (in contrast with a fresh sample), which is partially reversed by RT outgassing (Fig. 3c). This is similar to the quick and reversible generation of Ti<sup>3+</sup> not associated with anion vacancies observed by us earlier upon H<sub>2</sub> adsorption at RT on Rh/TiO<sub>2</sub> and similar systems (17, 18), which was ascribed to a reversible spillover of H atoms from the metal to the titania support with the final formation of Ti<sup>3+</sup> cations, the process depending on the location of the relevant Fermi levels. A similar particle-to-support electron transfer (but induced by CO adsorption) was proposed recently by us to occur on a RhO<sub>x</sub>/CeO<sub>2</sub> catalyst (19).

We think that the data reflected in Fig. 3 can be interpreted similarly in terms of reversible Au-TiO<sub>2</sub> electron transfer induced by CO adsorption, which would raise the Fermi level of the Au particle and thus lead to electron transfer from the latter to the oxide. Note that the *g* values of these Ti<sup>3+</sup> species differ from those found after adsorbing H<sub>2</sub> at RT on the cited M/TiO<sub>2</sub> catalysts, the latter values being then the same irrespective of the metal M involved (17); thus, an explanation of the present results in terms of H<sub>2</sub> formation from CO and surface OH groups (a water-gas shift type reaction) seems unlikely. It is worth noting that according to Fig. 2b some CO-induced electron transfer occurs here already at 77 K, with generation of a small amount of Ti<sup>3+</sup> bulk defects.

In relation to the fate of the electrons produced by reduction in these samples, it is worth commenting that, as shown in Figs. 1g and 1h, after the O<sub>2</sub> adsorption carried out in those experiments an increase is seen in the signals due to electron-containing bulk defects: that at *g* = 1.979, due to Ti<sup>3+</sup>, and that at *g* = 2.002, which in view of this behavior should be ascribed to vacancy-trapped electrons

and not just to organic impurities. There is not yet a clear explanation for this. Maybe some of the excess electrons still remaining after O<sub>2</sub> adsorption migrate to those defects because there are no more surface anion vacancy sites, but the influence of some other factor cannot be discarded.

#### *Consumption/Formation of Oxygenated Species on the TiO<sub>2</sub> Support upon CO Interaction*

Another point of interest refers to the different types of Ti<sup>3+</sup> EPR signal formed by the effect of CO in different situations. Thus, CO adsorption on fresh samples produces Ti<sup>3+</sup> of bulk defect type when carried out at 77 K (Fig. 2b); if performed at RT it gives additional Ti<sup>3+</sup> species associated with surface vacancies (Fig. 1g). The Ti<sup>3+</sup> centers formed (in larger amounts) upon CO adsorption on a sample which has been contacted with both CO and O<sub>2</sub> (data in Fig. 3) are not of the usual type associated with anion vacancies, but seem to have a more complete coordination sphere.

This means that a fresh (activated) catalyst sample contains O<sup>2-</sup> ions (probably, those most coordinatively unsaturated) which can be eliminated by CO adsorption (if Au is present to activate the molecule) leading to the formation of surface Ti<sup>3+</sup>-V<sub>O</sub> centers, but that such O<sup>2-</sup> ions are no longer present in the sample which has been in contact with both CO and O<sub>2</sub>; instead, other species, presumably formed as results of the interaction with CO and O<sub>2</sub>, are seemingly present which are not eliminated by CO adsorption at RT but remain at the coordination sphere of the corresponding Ti surface ions. These other oxygenated species could be of carbonate, peroxide, or some other EPR-undetectable species; the present results do not allow us to clarify this issue, and therefore they are just designated as X in line III (last stages) of Scheme 1, where this type of process is sketched. One may recall here that the presence of carbonate-type species has been detected by IR spectroscopy after interaction of CO + O<sub>2</sub> with Au/TiO<sub>2</sub> samples (20); they are therefore a plausible candidate for such X species. The large amplitude of the Ti<sup>3+</sup> signal detected under these conditions indicates that such species, acting as ligand of Ti ions, contribute to stabilize reduced states of these at the surface. The variety of Ti<sup>3+</sup> species detected in this case suggests that species X may exist in several ligating configurations, which again is compatible with their assignment to carbonate entities.

It is also worth noting that, while O<sub>2</sub> adsorption on a sample containing Ti<sup>3+</sup>-V<sub>O</sub> centers produces, besides the elimination of Ti<sup>3+</sup>, detectable amounts of Ti<sup>4+</sup>-stabilized O<sub>2</sub><sup>-</sup> radicals (Figs. 1f and 1h), in a sample which has (according to the discussion above) the surface covered with the mentioned species X a new O<sub>2</sub> adsorption (Figs. 3d and 3e) no longer produces detectable amounts of those radicals, even if Ti<sup>3+</sup> is effectively eliminated (which evidences that electron transfer to O<sub>2</sub> has indeed occurred). This indicates

that the hypothesized species X remaining on the surface Ti ions makes difficult the stabilization over these latter ions of  $O_2^-$  radicals, which therefore will further react more easily to give diamagnetic species. Note, on the other hand, that if  $O_2$  is adsorbed on a sample with CO adsorbed at 77 K but before warming it at RT,  $O_2^-$  radicals can be observed in significant amounts (Fig. 2c). This means that, when surface  $O^{2-}$  ions are not yet eliminated; i.e., when the more reactive  $Ti^{3+}$  ions with an important degree of coordinative insaturation are not formed, but species X have not yet been generated,  $O_2^-$  radicals can remain stable on  $Ti^{4+}$  ions. This situation is sketched in line III (third stage) of Scheme 1.

### Implications for the CO + O<sub>2</sub> Catalytic Reaction

The results presented show that interaction of CO with a fresh Au/TiO<sub>2</sub> catalyst at RT leads to reduction of the sample surface, via abstraction of surface  $O^{2-}$  ions by CO leading to the generation of  $Ti^{3+}$  anion vacancy complexes. Activation of the CO molecule on the Au particle is necessary for this, as well as for the other low-temperature reduction processes described here (note, however, that we cannot discard some influence on these processes of any structural modifications which may have occurred on the titania surface upon catalyst preparation, due e.g. to the calcination treatment, the presence of Au particle itself, or the action of  $Cl^-$  ions present during it; indeed the increase in the bulk defect EPR signals observed in the HCl-treated titania sample indicates that some such modifications may occur). Such an effect of CO adsorption suggests an important role of the titania  $O^{2-}$  surface ions in the reaction mechanism. However, while this may be true for the initial contact of the reacting mixture with the catalyst, the state of the latter during the steady state reaction is probably more similar to that prevalent in the experiments of Figs. 4b–4d, in which the sample has been in contact with both CO and  $O_2$  at RT. The discussion above indicates that in this case the surface is largely covered by adsorbed reaction products (at least in the region close to the Au particles) which are not abstracted by CO; then  $Ti^{3+}-V_O$  centers do not appear, and Ti cation-stabilized  $O_2^-$  is not observed. This does not mean that  $O_2^-$  is not formed, but rather that it further reacts quickly to give diamagnetic species. The transfer of electrons to  $O_2$  may take place from the Au particle itself, as shown by the results obtained on Au/Al<sub>2</sub>O<sub>3</sub> (which is able as well to catalyze the CO +  $O_2$  reaction (3)), but in the case of Au/TiO<sub>2</sub> it might occur also (with lower activation

energy) through Ti ions, thanks to the easy Au-to-TiO<sub>2</sub> electron transfer which appears to occur stimulated by CO adsorption. Of course, depending on their precise nature these titania-adsorbed species generically designated as X might be reactive at higher temperatures and/or toward other reactants such as H<sub>2</sub> or organic molecules.

### ACKNOWLEDGMENTS

The authors appreciate a Grant-in-Aid from the Japanese Science and Technology Agency for the international joint research program. J.M.C. appreciates a postdoctoral grant from the Comunidad Autónoma de Madrid.

### REFERENCES

1. Haruta, M., Tsubota, S., Kobayashi, T., Kageyama, H., Genet, M. J., and Delmon, B., *J. Catal.* **144**, 175 (1993).
2. Haruta, M., Yamada, N., Kobayashi, T., and Iijima, S., *J. Catal.* **115**, 301 (1989).
3. (a) Okumura, M., Nakamura, S., Tsubota, S., Nakamura, T., Azuma, M., and Haruta, M., *Catal. Lett.* **51**, 53 (1998); (b) Okumura, M., Tsubota, S., Iwamoto, M., and Haruta, M., *Chem. Lett.* 315 (1998).
4. Okumura, M., and Haruta, M., *Chem. Lett.* 396 (2000).
5. Gardner, S. D., Hoflund, G. B., Upchurch, B. T., Schryer, D. R., Kielin, E. J., and Schryer, J., *J. Catal.* **129**, 114 (1991).
6. Knell, A., Barnickel, P., and Wokaun, A., *J. Catal.* **137**, 306 (1992).
7. Tsubota, S., Cunningham, D. A. H., Bando, Y., and Haruta, M., in "Preparation of Catalysts VI" (G. Poncelet *et al.*, Eds.), pp. 227–235. Elsevier, Amsterdam, 1995.
8. Kobayashi, T., Haruta, M., Tsubota, S., and Sano, H., *Sensors Actuators B1*, 222 (1990).
9. (a) Haruta, M., *Catal. Today* **36**, 153 (1996); (b) *Catal. Surveys Jpn.* **1**, 61 (1997).
10. (a) Haruta, M., Kobayashi, T., Tsubota, S., and Nakahara, Y., *Chem. Express* **3**, 159 (1988); (b) Tsubota, S., Haruta, M., Kobayashi, T., Ueda, A., and Nakahara, Y., in "Preparation of Catalysts V" (G. Poncelet *et al.*, Eds.), pp. 695–704. Elsevier, Amsterdam, 1991.
11. Meriaudeau, P., Che, M., Gravelle, P. C., and Teichner, S., *Bull. Soc. Chim. Fr.* 13 (1971).
12. Che, M., and Tench, A. J., *Adv. Catal.* **32**, 1 (1983).
13. Soria, J., Martínez-Arias, A., and Conesa, J. C., *J. Chem. Soc., Faraday Trans.* **91**, 1669 (1995).
14. Che, M., Gravelle, P. C., and Meriaudeau, P., *C. R. Acad. Sci. Paris C* **268**, 768 (1969).
15. Abragam, A., and Bleaney, B., "Electron Paramagnetic Resonance of Transition Ions." Clarendon, Oxford, 1970.
16. Bruce Losee, D., *J. Catal.* **50**, 545 (1977).
17. Conesa, J. C., and Soria, J., *J. Phys. Chem.* **86**, 1392 (1982).
18. Conesa, J. C., Soria, J., Rojo, J. M., Sanz, J., and Munuera, G., *Z. Phys. Chem. Neue Folge* **152**, 83 (1987).
19. Martínez-Arias, A., Conesa, J. C., and Soria, J., *J. Catal.* **168**, 364 (1997).
20. Boccuzzi, F., Chiorino, A., Manzoli, M., Andreeva, D., and Tabakova, T., *J. Catal.* **188**, 176 (1999).